



## Thermal analysis of formation of nano-crystalline BaTiO<sub>3</sub> using Ba(NO<sub>3</sub>)<sub>2</sub> and TiO<sub>2</sub>

Md. Jawed Ansaree, Shail Upadhyay\*

Department of Physics, Indian Institute of Technology, Banaras Hindu University, Varanasi - 221 005, U. P. India

Received 14 August 2015; Received in revised form 20 November 2015; Accepted 29 November 2015

### Abstract

The reaction of Ba(NO<sub>3</sub>)<sub>2</sub> with TiO<sub>2</sub> was studied by thermogravimetric (TG) and differential scanning calorimetric (DSC) techniques up to 1000 °C and in nitrogen atmosphere. It was found that the formation of BaTiO<sub>3</sub> takes place above 600 °C and that precursor mixing time and heating rate have no effect on the reaction temperature. BaTiO<sub>3</sub> powder was prepared by calcination of Ba(NO<sub>3</sub>)<sub>2</sub> and TiO<sub>2</sub> precursor mixture at 800 °C for 8 h. X-ray diffraction analysis of the synthesized BaTiO<sub>3</sub> confirmed the formation of tetragonal phase with lattice parameters  $a = 3.9950 \pm 0.0003 \text{ \AA}$  and  $c = 4.0318 \pm 0.0004 \text{ \AA}$ . Thermal analysis of the synthesized BaTiO<sub>3</sub> powder showed weight loss within temperature range 40–1000 °C of only 0.40%. This small amount of weight loss was connected with some impurity phase, and identified as BaCO<sub>3</sub> using Fourier transform infrared (FTIR) technique.

**Keywords:** synthesis, barium titanate, Ba(NO<sub>3</sub>)<sub>2</sub> precursor, thermal analysis, XRD, FTIR

### I. Introduction

Performance of BaTiO<sub>3</sub> ceramics significantly depends on the microstructure of the sintered body, which is influenced by characteristics of the starting BaTiO<sub>3</sub> powder. Therefore, much attention has been focused on the synthesis of high quality BaTiO<sub>3</sub> nano-particles and different techniques have been used: sonochemical synthesis [1], sol-gel [2], hydrothermal [3], solvothermal [4], chemical co-precipitation [5] and supercritical fluid [6]. These methods are not cost-effective in mass production of BaTiO<sub>3</sub> nanopowders. Thus, preparation of BaTiO<sub>3</sub> powders, using solid state reaction synthesis is regarded as one of the most practical and economical ways [7]. However, in the conventional solid phase methods, BaTiO<sub>3</sub> powders were usually produced via the reaction between the mechanically mixed BaCO<sub>3</sub> or BaO and TiO<sub>2</sub> powders followed by calcination at above 1000 °C [8]. Unfortunately, the reactions at such high temperatures are beyond control and the resultant powders often have large particle size and wide particle size distribution. Therefore, for industrial applica-

tions, it is still desirable to develop an alternative low-temperature solid state method for the preparation of nano-crystalline BaTiO<sub>3</sub> powders at low cost.

Researchers have tried to synthesize BaTiO<sub>3</sub> powders at lower temperatures by replacing BaCO<sub>3</sub> by other compounds such as Ba(OH)<sub>2</sub>, Ba(COO<sub>2</sub>), Ba(NO<sub>3</sub>)<sub>2</sub> etc. [9]. Thus, it was reported that the reaction of Ba(NO<sub>3</sub>)<sub>2</sub> with TiO<sub>2</sub> (anatase) yielded the single phase BaTiO<sub>3</sub> at much lower temperatures, around 600 °C [10–12], but this method has not been studied in details like a synthesis of BaTiO<sub>3</sub> using BaCO<sub>3</sub> and TiO<sub>2</sub>. Therefore, the aim of this work is to study the formation of BaTiO<sub>3</sub> from Ba(NO<sub>3</sub>)<sub>2</sub> and TiO<sub>2</sub>, using thermogravimetric (TG) and differential scanning calorimeter (DSC) analysis. Further characterization of the prepared BaTiO<sub>3</sub> powder was done using thermal analysis (TG and DSC), X-ray diffraction (XRD) and Fourier Transform Infra-red (FTIR) techniques.

### II. Experimental

#### 2.1. Sample preparation

BaTiO<sub>3</sub> powder was prepared by using Ba(NO<sub>3</sub>)<sub>2</sub> (purity 99%, Qualikens, USA) and titanium dioxide (rutile TiO<sub>2</sub> purity 99.5%, Alfa Aesar, UK) as the starting

\*Corresponding author: tel: +91 5426701919, fax: +91 9889446217, e-mail: supadhyay.app@itbhu.ac.in, shail72@yahoo.com

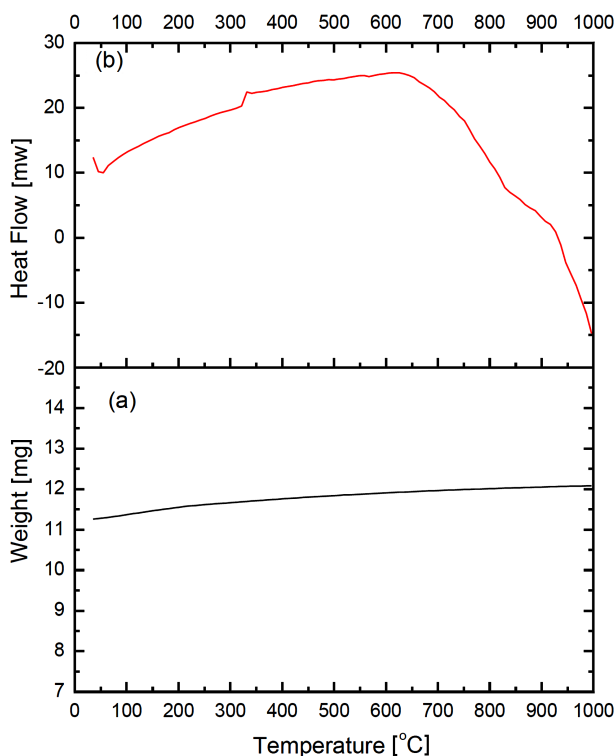


Figure 1. TG (a) and DSC curves (b) of  $\text{TiO}_2$

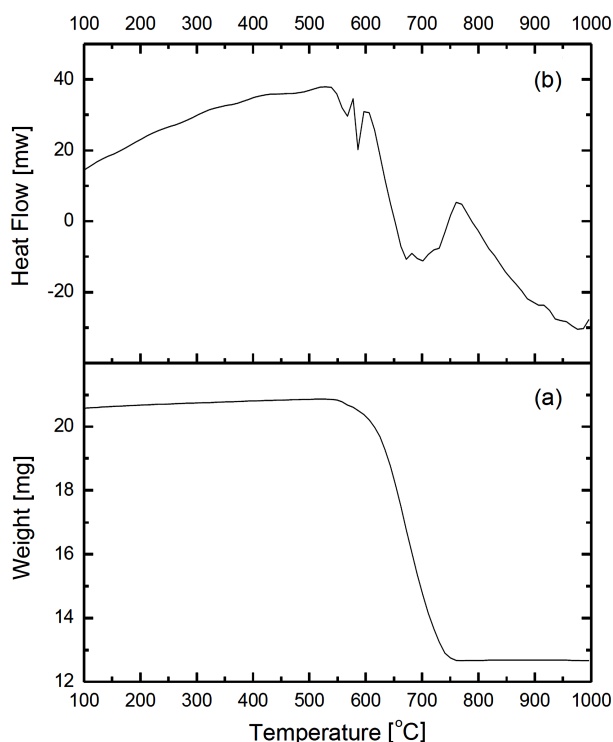


Figure 2. TG (a) and DSC curves (b) of  $\text{Ba}(\text{NO}_3)_2$

materials. Equi-molar amounts of  $\text{Ba}(\text{NO}_3)_2$  and  $\text{TiO}_2$  powders were crushed in agate mortar for 3 hours. The mixture was transferred to an alumina crucible and calcined in a furnace (Matrix, India) at  $800^\circ\text{C}$  for 8 h with a heating rate of  $10^\circ\text{C}/\text{min}$  and after that the furnace was cooled down to room temperature.

## 2.2. Characterization techniques

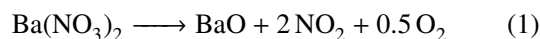
Thermal analysis (TG and DSC) of the reactants, precursor mixture of reactants and synthesized powders were carried out by using simultaneous TG-DSC (Mettler Toledo, Germany) thermal analyzer in the temperature range  $30\text{--}1000^\circ\text{C}$  with heating rates of 10 and  $20^\circ\text{C}/\text{min}$  in nitrogen atmosphere. A preliminary study on compound formation and lattice parameters was carried out by using X-ray diffraction (XRD) technique with an X-ray powder diffract meter (Miniflex, Rigaku). Fourier transform infrared (FTIR) spectra of the sample were recorded by using Fourier Transform Infra-red Spectrometer (Shimadzu, Model DF 803) in the wave number range  $400\text{--}4000\text{cm}^{-1}$ .

## III. Results and discussion

### 3.1. Thermal analysis of $\text{TiO}_2$ and $\text{Ba}(\text{NO}_3)_2$

The TG and DSC curves of  $\text{TiO}_2$  powder with a heating rate of  $10^\circ\text{C}/\text{min}$  in nitrogen atmosphere are shown in Figs. 1a and 1b, respectively. No weight change and peaks have been observed in the TG and DSC curves of  $\text{TiO}_2$  powder in the temperature range  $30\text{--}1000^\circ\text{C}$ .

The TG and DSC curves of  $\text{Ba}(\text{NO}_3)_2$  are shown in Figs. 2a and 2b, respectively. The TG curve shows a single step weight loss (approximately 41%) in the temperature range  $550\text{--}725^\circ\text{C}$ . It was reported [13] that anhydrous bulk barium nitrate decomposes over the temperature range  $500\text{--}700^\circ\text{C}$ , with the main decomposition taking place at  $630^\circ\text{C}$ . Slightly higher decomposition temperature range observed for nitrate used in this work may be due to difference in the particle size. The observed weight loss is in good agreement with the theoretical weight loss calculated according to the reaction (1):



The DSC curve of  $\text{Ba}(\text{NO}_3)_2$  shows two peaks at  $587^\circ\text{C}$  and  $708^\circ\text{C}$ . The first peak is attributed to the melting of  $\text{Ba}(\text{NO}_3)_2$  whereas the second peak to the decomposition of  $\text{Ba}(\text{NO}_3)_2$  to  $\text{BaO}$  according to the reaction (1). The observed melting temperature is approximately the same as reported value of  $592^\circ\text{C}$  [14].

### 3.2. Thermal analysis of $\text{Ba}(\text{NO}_3)_2/\text{TiO}_2$ mixture

Figures 3 and 4 show the TG and DSC curves, respectively, of the mixture of  $\text{Ba}(\text{NO}_3)_2$  and  $\text{TiO}_2$  obtained upon heating with two different rates (10 and  $20^\circ\text{C}/\text{min}$ ) and for two different mixing times (1 and 3 hours). There is no significant change in the nature of TG curves with variations in the heating rate and mixing time. All three TG curves show a single step weight loss (approximately 31%) between  $550\text{--}625^\circ\text{C}$ . The formation of  $\text{BaTiO}_3$  perovskite phase, in single step accompanied by the release of  $\text{NO}_2$  and  $\text{O}_2$  gases, takes place according to the following equation:



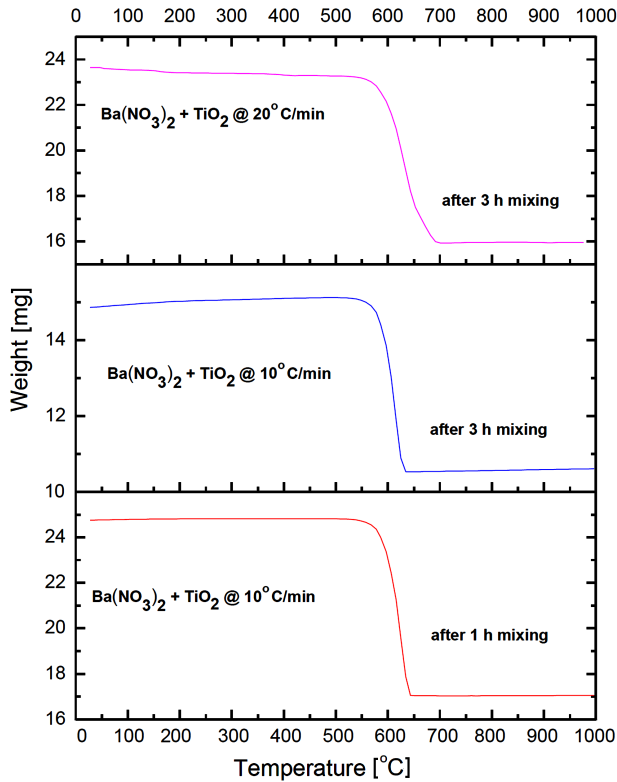


**Figure 3.** TG curves (obtained with different heating rates) of the mixture of  $\text{Ba}(\text{NO}_3)_2 + \text{TiO}_2$  prepared by different mixing times

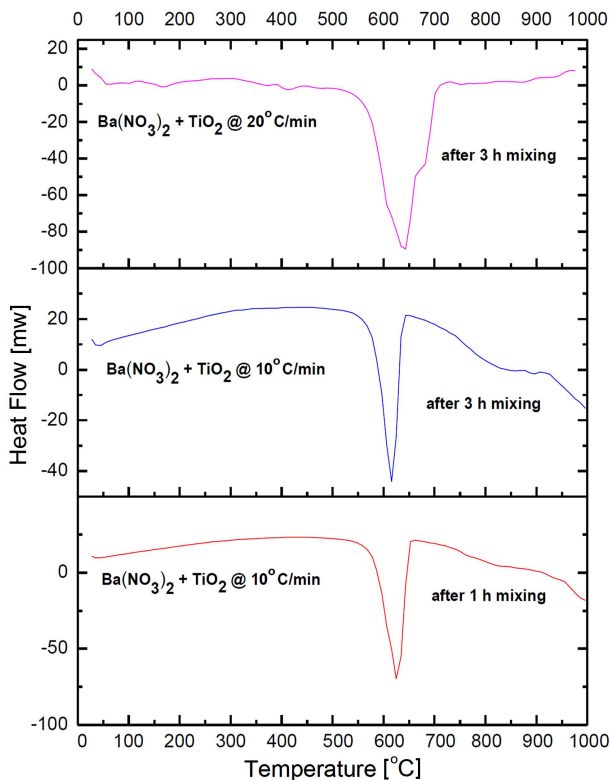


**Figure 4.** DSC curves (obtained with different heating rates) of the mixture of  $\text{Ba}(\text{NO}_3)_2 + \text{TiO}_2$  prepared by different mixing times

The weight loss of 31% observed experimentally is in agreement with the theoretical weight loss calculated according to the reaction (2).

DSC curves show only one endothermic peak between 610–650 °C. Since this peak is above the melting temperature of  $\text{Ba}(\text{NO}_3)_2$  it is attributed to the liquid-solid reaction between  $\text{Ba}(\text{NO}_3)_2$  and  $\text{TiO}_2$  during the formation of  $\text{BaTiO}_3$ . Observations of a single peak in the DSC curve contradict to the results reported by other workers. Tagawa *et al.* [10] have observed two endothermic peaks in the DTA curve. They attributed the first peak, at ~600 °C, to the melting of  $\text{Ba}(\text{NO}_3)_2$  and the second one, at ~650 °C, to the reaction of  $\text{Ba}(\text{NO}_3)_2$  with  $\text{TiO}_2$ . They concluded that the reaction occurs in the liquid-solid phase after the melting of  $\text{Ba}(\text{NO}_3)_2$  at high heating rates (10 and 20 °C/min). Othman *et al.* [12] showed that the reaction between  $\text{Ba}(\text{NO}_3)_2$  and  $\text{TiO}_2$  proceeds during heating up in three consecutive stages, characterized by three endothermic peaks at 605, 633.7 and 675.2 °C in the DTA curve. The first peak (at 605 °C) might be attributed to the solid-solid reaction between  $\text{Ba}(\text{NO}_3)_2$  and  $\text{TiO}_2$  powders. The second peak (at 633.7 °C) is due to the reaction between the partially melted  $\text{Ba}(\text{NO}_3)_2$  and  $\text{TiO}_2$ . The last endothermic peak (at 675.2 °C) is due to the complete reaction of the molten  $\text{Ba}(\text{NO}_3)_2$  with the residual  $\text{TiO}_2$ .

### 3.3. Characterization of synthesized $\text{BaTiO}_3$ powder

Figure 5 shows TG-DSC curves of the synthesized  $\text{BaTiO}_3$  powder, obtained after calcination at 800 °C for 8 h at a heating rate of 10 °C/min in nitrogen atmosphere. The TG curve depicts only 0.4% weight loss below 800 °C which could be attributed to the decomposition of a small amount of an impurity phase. There is no distinct peak in the DSC curve of the obtained powder which reflects high purity and thermal stability of the synthesized material.

The X-ray diffraction (XRD) pattern of synthesized  $\text{BaTiO}_3$  powder is shown in Fig. 6 and confirms the formation of  $\text{BaTiO}_3$ . The crystal structure of  $\text{BaTiO}_3$  powder is tetragonal (JCPDS No. 15-0780) because both 200 and 002 peaks (around  $2\theta = 45^\circ$ ) are present in the XRD pattern (see the inset of Fig. 6). The lattice parameters obtained using software “Cell” are  $a = 3.9950 \pm 0.0003 \text{ \AA}$  and  $c = 4.0318 \pm 0.0004 \text{ \AA}$ . The value of the tetragonality calculated using these values of lattice parameters is 1.0092 which is slightly smaller than standard value 1.0110. This may be due to the lower synthesis temperature used. It is reported that tetragonality of  $\text{BaTiO}_3$  is a function of temperature and standard value of tetragonality can be achieved after sintering at temperature >1300 °C [15].

The average crystallite size of the synthesized  $\text{BaTiO}_3$  powder was calculated from the X-ray line broadening of the 110 peak using Scherrer’s formula:

$$D = \frac{0.9\lambda}{\beta \cos \theta_{max}} \quad (3)$$

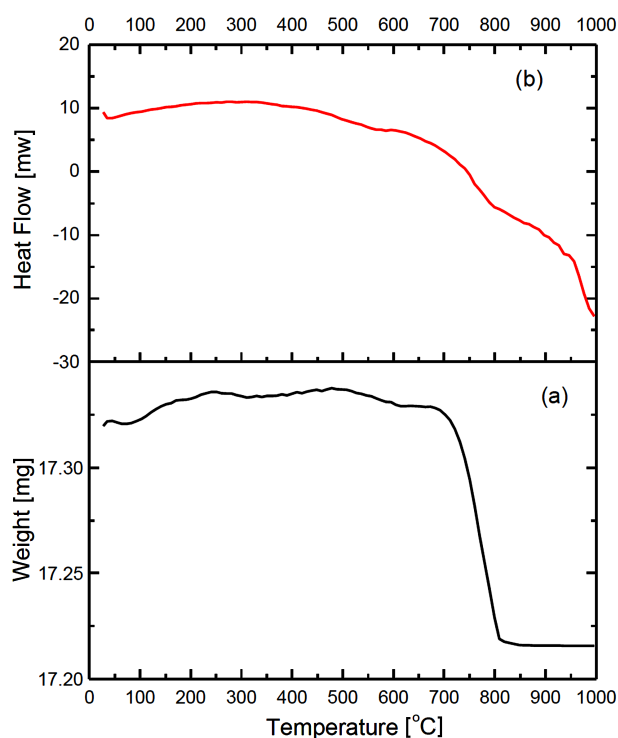


Figure 5. TG (a) and DSC curve (b) of synthesized BaTiO<sub>3</sub> powder

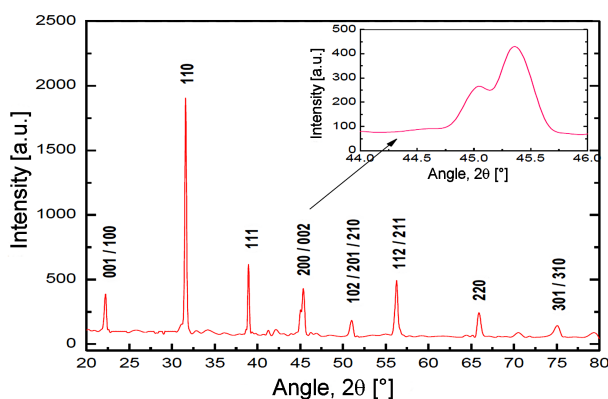


Figure 6. X-ray diffraction pattern of synthesized BaTiO<sub>3</sub> powder

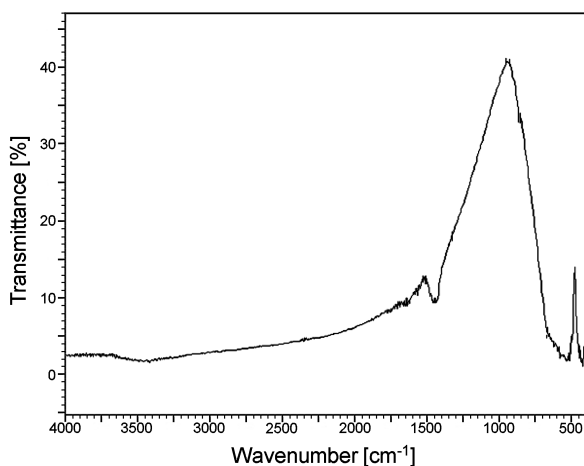


Figure 7. FTIR spectrum of synthesized BaTiO<sub>3</sub> powder

where  $D$  is the average grain size,  $\lambda = 1.541 \text{ \AA}$  (X-ray wavelength), and  $\beta$  is the width of the diffraction peak at half maximum for the diffraction angle  $2\theta$ . The average particle size is found to be 44 nm.

According to the reported literatures, BaCO<sub>3</sub> is the most common impurity of the BaTiO<sub>3</sub> powder prepared by any method. FTIR was found to be the most sensitive technique for the detection of BaCO<sub>3</sub>. On the basis of FTIR analysis, BaCO<sub>3</sub> concentration down to 0.6% has been estimated. In order to check the purity of the obtained BaTiO<sub>3</sub> powder, FTIR spectra of the sample is recorded and shown in Fig. 7. The crystallization of barium titanate was confirmed by the broad band centered at 540 cm<sup>-1</sup>, which is typical of the Ti–O stretching vibrations in BaTiO<sub>3</sub>, and also by the second broad band observed at the end of the spectra, below 500 cm<sup>-1</sup>, corresponding to the Ti–O bending vibrations [16]. The very small absorption band at 1440 cm<sup>-1</sup> can be interpreted as C=O vibration due to extremely small unavoidable traces of carbonate [17]. This result is contradictory to the result obtained by XRD (Fig. 6 in which no peak of BaCO<sub>3</sub> is observed), but is in agreement with results obtained by TG curve (Fig. 5). From the TG it was found that amount of impurity phase BaCO<sub>3</sub> is approximately 0.4% and as it could be expected XRD is unable to detect such small amount of BaCO<sub>3</sub> impurity phase.

#### IV. Conclusions

The BaTiO<sub>3</sub> powder was synthesized from Ba(NO<sub>3</sub>)<sub>2</sub> and TiO<sub>2</sub> powder mixture with 1:1 molar ratio. The TG-DSC results showed that the reaction between Ba(NO<sub>3</sub>)<sub>2</sub> and TiO<sub>2</sub> proceeds during heating up in single stage (above 600 °C) between molten Ba(NO<sub>3</sub>)<sub>2</sub> with TiO<sub>2</sub> (liquid-solid reaction). The TG-DSC results showed that the formation of BaTiO<sub>3</sub> phase from Ba(NO<sub>3</sub>)<sub>2</sub> and TiO<sub>2</sub> powder mixture takes place before Ba(NO<sub>3</sub>)<sub>2</sub> decomposes to BaO. X-ray diffraction pattern of the synthesized BaTiO<sub>3</sub> obtained after calcining mixture of BaTiO<sub>3</sub> and TiO<sub>2</sub> at 800 °C for 8 h confirmed the formation of tetragonal phase with lattice parameters  $a = 3.9950 \pm 0.0003 \text{ \AA}$  and  $c = 4.0318 \pm 0.0004 \text{ \AA}$ . The obtained powder has crystallite size of 44 nm. The purity of the obtained powder has been checked by thermal characterization (TG and DSC). Only 0.40% weight loss has been detected within temperature range 40–1000 °C. This small amount of impurity phase was identified as BaCO<sub>3</sub> using Fourier transform infra-red (FTIR) technique.

**Acknowledgements:** The authors gratefully acknowledge the financial support provided by Defense Research and Development Organization (DRDO), New Delhi, India through research project ERIP/ER/1000387/M/01/1418. Authors are also thankful to the Head of the Department, Pharmaceutics, IIT (BHU) for providing FTIR facility.

## References

1. M. Xu, Y. Lu, Y. Liu, S. Shi, T. Qian, D. Lu, “Sonochemical synthesis of monosized spherical BaTiO<sub>3</sub> particles”, *Powder Technol.*, **161** (2006) 185–189.
2. X. Xing, J. Deng, J. Chen, G. Liu, “Phase evolution of barium titanate from alkoxide gel-derived precursor”, *J. Alloys Compd.*, **384** (2004) 312–317.
3. L. Wang, H. Kang, K. Li, D. Xue, C. Liu, “Phase evolution of BaTiO<sub>3</sub> nanoparticles: An identification of BaTi<sub>2</sub>O<sub>5</sub> intermediate phase in calcined stearic acid gel”, *J. Phys. Chem. C*, **112** (2008) 2382–2388.
4. C. Bi, M. Zhu, Q. Zhang, Y. Li, H. Wang, “Electromagnetic wave absorption properties of multi-walled carbon nanotubes decorated with La-doped BaTiO<sub>3</sub> nano crystals synthesized by a solvothermal method”, *Mater. Chem. Phys.*, **126** (2011) 596–601.
5. G.J. Choi, S.K. Lee, K.J. Woo, K.K. Koo, Y.S. Cho, “Characteristics of BaTiO<sub>3</sub> particles prepared by spray co-precipitation method using titanium acylate-based precursors”, *Chem. Mater.*, **10** (1998) 4104–4113.
6. G. Philippot, C. Elissalde, M. Maglione, C. Aymonier, “Supercritical fluid technology: A reliable process for high quality BaTiO<sub>3</sub> based nanomaterials”, *Adv. Powder Technol.*, **25** (2014) 1415–1429.
7. A. Ioachim, M.I. Toacsan, M.G. Banciu, L. Nedelcu, F. Vasiliu, H.V. Alexandru, C. Berbecaru, G. Stoica, “Barium strontium titanate-based perovskite materials for microwave applications”, *Prog. Solid State Chem.*, **35** (2007) 513–520.
8. K.I. Othman, A.A. Hassan, A. Omar, A. Abdelal, E.S. Elshazly, M. El-Sayed Ali, S.M. El-Raghy, S. El-Houte, “Formation mechanism of barium titanate by solid-state reactions”, *Int. J. Sci. Eng. Res.*, **5** [7] (2014) 1460–1465.
9. H. Tagawa, J. Ohashi, “Formation of barium titanate: Reactivity of raw materials”, *Denki Kagaku*, **52** (1984) 485–490.
10. H. Tagawa, J. Ohashi, “Kinetics and mechanism of the reaction of Ba(NO<sub>3</sub>)<sub>2</sub> and TiO<sub>2</sub> (anatase) in the solid-solid state and the liquid-solid state”, *Thermochem. Acta*, **88** (1985) 307–312.
11. S.Z. Liu, T.X. Wang, L.Y. Yang, “Low temperature preparation of nanocrystalline SrTiO<sub>3</sub> and BaTiO<sub>3</sub> from alkaline earth nitrates and TiO<sub>2</sub> nanocrystals”, *Powder Technol.*, **212** (2011) 378–381.
12. K.I. Othman, A.A. Hassan, M. El-Sayed Ali, M.E. Raghy, R.A. Karim, O.A. Abdetal, F.E. Zhraa, S.E. Dien, “Characterization and dielectric properties of BaTiO<sub>3</sub> prepared from Ba(NO<sub>3</sub>)<sub>2</sub>-TiO<sub>2</sub> mixture”, *J. Rad. Res. Appl. Sci.*, **5** (2012) 15–25.
13. C.J. Bardwell, R.I. Bickley, S. Poulston, M.V. Twigg, “Thermal decomposition of bulk and supported barium nitrate”, *Thermochim. Acta*, **613** (2015) 94–99.
14. D.E. Perry, *Hand Book of Inorganic Compounds*, Second edition, CRC Press, 2011.
15. L.B. Kong, J. Ma, H. Huang, R.F. Zhang, W.X. Que, “Barium titanate derived from mechanochemically activated powders”, *J. Alloys Compd.*, **337** (2002) 226–230.
16. H. Reverón, C. Aymonier, A. Loppinet-Serani, C. Elissalde, M. Maglione, F. Cansell, “Single-step synthesis of well-crystallized and pure barium titanate nanoparticles in super critical fluids”, *Nanotechnol.*, **16** (2005) 1137–1143.
17. L. Wang, H. Kang, K. Li, D. Xue, C. Liu, “Phase evolution of BaTiO<sub>3</sub> nanoparticles: an identification of BaTi<sub>2</sub>O<sub>5</sub> intermediate phase in calcined stearic acid gel”, *J. Phys. Chem. C*, **112** (2008) 2382–2388.

